Profile Measurement of Rails in a Rolling Mill: Implementing and Evaluating Autonomic Computing Capabilities

Álvaro F. Millara, Julio Molleda*, Rubén Usamentiaga, Daniel F. García, *Member, IEEE*
Department of Computer Science and Engineering, University of Oviedo, Spain
*Corresponding author email address: jmolleda@uniovi.es

***Abstract*—Profile measuring is a key data acquisition process in the rail manufacturing industry. In rail rolling mills, profile measurement systems inspect the shape of the rail profiles to assess their dimensional quality. This assessment can be used in order to provide feedback for shape control devices in upstream manufacturing, and also to check whether the products are compliant with rail standards and client requirements. This paper deals with designing autonomic computing capabilities, specifically self-awareness, to a rail profile measurement system based on laser range finding, and then evaluating their suitability for the following tasks: *i*) automatically detect changes in both the working environment and the operating conditions; and *ii*) warn process computers and operators of the rail rolling mill when working conditions indicate that the accuracy of the inspection system has fallen below a given threshold.**

Keywords*—Autonomic computing; self-awareness; dimensional assessment; shape inspection; machine vision.

I. Introduction

Steel rails are used to build rail tracks for wheeled vehicles to transport both cargo and passengers over short and long distances, and also to manipulate cargo in heavy industry and warehousing. Rails are engineered, designed and produced to support high-speed, heavily loaded modern trains. The typical manufacturing process involves several stages [1]. First, iron core is reduced in blast furnaces. Then liquid iron is refined by means of controlled oxidation of carbon and other elements in steelmaking vessels called converters. After the basic steelmaking oxygen conversion, secondary steelmaking is performed in arc furnaces, where the desired steel composition is achieved by adding alloying elements to the molten steel. The bloom undergoes a continuous casting process where oxide inclusions are removed to achieve the required structural integrity. It is then reheated and passed through a series of rolling cages, which progressively shape it into a rail. Finally, the resulting rail is sawed and cooled.

In order to ensure the safety and quality of rail transportation, rail inspection is performed in two different scenarios to assess whether the rail successfully fulfills the required standards and the requirements of the clients [2]: *i*) the rolling mill, where continuous monitoring of rail profiles during rail manufacturing is used to assess flatness [3], surface [4] and dimensions [5] of the rails; and *ii*) the railroad, where rail profile measurements are used to inspect the wear and tear of the rail track.

In rail rolling mills, consistent rail dimensions and surface quality are ensured by tight control of rolling temperatures. Processing speeds in these mills are ever increasing, pushing on-line sensors to meet very narrow deadlines. In addition, current international standards impose strict tolerances on rails, which means that these sensors require high levels of accuracy. In the rolling process, dimensional inspection of rail profiles is essential to provide precise feedback to upstream rolling stages and to ensure the rails meet the required standards for modern high speed and heavy-haul networks.

In general, profile measurement systems in rail rolling mills are based on active triangulation through laser range finding. Other optical techniques, such as fringe pattern projection, could potentially be used. However, such techniques require a more complex setup, and typically present a higher computational cost [6], which makes their use inadvisable for tasks where laser triangulation suffices.

Laser triangulation systems are typically installed in housings to provide a controlled lighting environment and to prevent human operators from being exposed to laser reflections. These installations may not be accessed by human operators when the rolling mill is in operation. In addition, the 24/7 service goal of modern manufacturing lines means that they cannot be stopped to check instrumentation, except for scheduled maintenance stops. This makes on-line performance evaluation of these systems difficult. On the contrary, some active triangulation systems provide off-line performance evaluation [7], [8]. Tests run on these systems may show possible measurement errors, and maintenance policies can be defined when these errors are larger than a defined threshold. Other off-line methods allow compensating measurement errors through error characterization [9].

Autonomic computing refers to the self-management of the resources of a computing system [10], [11]. Self-management implies: *i*) self-configuration of the system for a certain usage or a specific platform or user; *ii*) self-optimization of the system and its use of resources, both reactively and proactively; *iii*) self-healing of the system, which includes problem detection, diagnostic and, when possible, repair; and *iv*) self-protection of the system against security threats, both malicious and not. In order to achieve these abilities, policies describing the desired system conditions must be defined. These policies determine how the effectors of the system should be used in order to correct its operation. Such decisions must be based on the properties of the system, which are measured by a series of sensors. The basic structure of an autonomic system

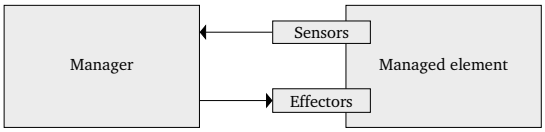

Fig. 1. Basic structure of an autonomic system.

can be seen in Fig. 1. Thus, a managed element (or a set or managed elements) exposes sensors and effectors to an autonomic manager, which implements the autonomic features. The system conformed by the managed element or elements and the manager is called an autonomic system.

This work deals with the design of autonomic computing capabilities, which run on-line with no human intervention, for rail profile measurement systems in rolling mills based on active triangulation with two main goals. First, to detect changes in the environment that could lead to malfunction of the system. Second, to warn process computers and operators of the rail rolling mill when working conditions indicate that the system is about to provide incorrect measurements. The autonomic computing procedures proposed in this paper add self-awareness capabilities [12], i.e. self-inspection and self-decision, to the system. These procedures characterize the laser patterns projected onto the surface of rails to determine degradation on the system performance and changes in the working environment. This approach is built on our previous works [5], [13], where we designed and developed a rail profile measurement system for rail rolling mills and we proposed the integration of autonomic computing capabilities.

This paper is organized as follows: Section II describes the state of the art and our previous work. Section III describes features of the light patterns that are useful for the purpose of implementing autonomic capabilities. Section IV explains the design and implementation of said autonomic capabilities. Section V describes the experiments that were carried out on the available image database and Section VI comments on their results. Finally, our conclusions are stated in Section VII.

II. Rail profile measurement using machine vision

Profile measurement systems provide 3D information about the shape of an object. In recent decades, many different optical techniques have been proposed to measure the surface of manufactured products [14]. These techniques are classified into passive and active [15]. The former project light patterns onto the surface of the product under inspection, whereas the latter only require environmental light of the scene. Among them, active triangulation is the most commonly used in industrial environments since it provides the best relation between accuracy and cost.

A. Active triangulation using laser range finding

Optical sensors in industry tend to use controlled lighting methods, that is, active methods, to avoid external noise when they are installed in hostile environments. The most commonly used method for contactless profile measurement in the steelmaking industry is active triangulation.

Laser range finding is a method for determining the surface profile of an object at a given section using laser triangulation. The laser pattern generator is mounted perpendicular to the surface under inspection, whereas the camera images the intersection of the sheet-of-light with the surface at an angle, α, called the triangulation angle. This angle determines the measuring area and the resolution of measurements. Using the mathematical camera model, together with the geometry of the system, the distorted pattern imaged by the camera can be translated into the world coordinate system. In this way, the 3D height profile of the object can be provided.

B. Profile measurement in rail rolling mills

Rail inspection systems can be classified into two categories: *i*) contact systems, which use mechanical devices and apply tactile techniques to indirectly observe the rail geometry [16]; and *ii*) non-contact systems, mainly based on automated visual inspection using structured light [17], [18].

In previous works we developed a machine-vision-based, non-contact profile measurement system (PMS) of rails for a rail rolling mill [5]. This system provides on-line measurements of several dimensions of rails based on geometric parameters of the transverse sections, also called profiles, of the rails. The PMS is based on active range imaging, specifically on laser triangulation, using four coupled laser range finders, similar to those used in other applications in the metal industry [19]. The geometry of this system is shown in Fig. 2, where each pair $\{C_i, L_i\}$, $i \in [1, 4]$ represents a laser range finder, also referred as a laser triangulation unit.

Experiments carried out both in the lab and in a rail rolling mill demonstrate that the PMS provides accurate and repeatable measurements [5]. This measurement system is able to accurately inspect the dimensional quality of rails in the mill using conventional, inexpensive machine vision components.

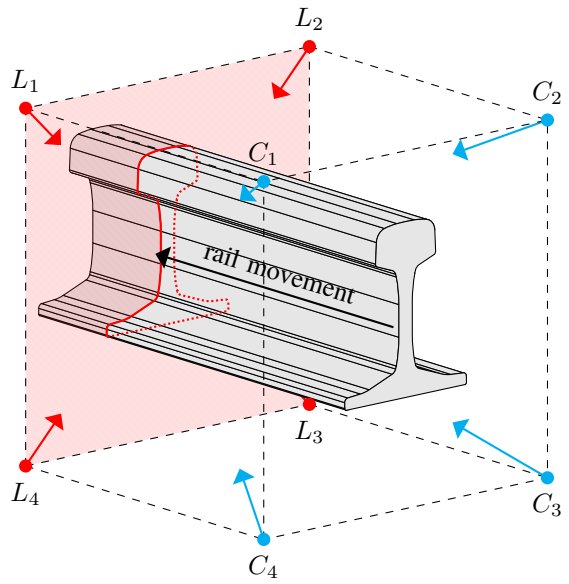

Fig. 2. Geometry of the rail profile measurement system used in this work: C_1, C_2, C_3 and C_4 represent the image sensors whereas L_1, L_2, L_3 and L_4 represent the laser emitters. The distances depicted in this figure are not to scale.

This system is based on a high-performance software architecture, using pipelining and parallelism to meet real-

time constraints imposed by on-line monitoring. The system is divided into five main stages: *i*) image acquisition; *ii*) laser line detection and extraction; *iii*) 2D to 3D coordinate translation; *iv*) 3D rail profile computation; and *v*) dimensional measurement of the rail profile.

From the measurement point of view, the key stage of this PMS is laser line detection and extraction. Laser line extraction is a straightforward task under controlled conditions of surrounding light and laser power [20]. However, common line extraction methods are highly sensitive to noise and they have major problems in industrial environments. In harsh environments a robust and accurate method capable of dealing with variable luminance, uneven surfaces and reflections which show up in images as noise is required [21]. Our rail PMS extracts the single-line pattern projected onto the rail surface using a procedure based on a well-known differential geometric algorithm [22].

III. Light pattern characterization

One of the most important features of an inspection system based on laser triangulation is the light patterns projected onto the surface of the product under inspection, which allow for the retrieval of the 3D shape of the product surface. This shape is then translated to the world coordinate system in order to compute a set of measurements. These measurements make up the inputs for high level layers of the system, allowing, for instance, deciding whether the inspected product fulfils the requirements of a client or whether it is compliant with a given standard. Therefore, laser patterns provided by the image acquisition subsystem of a laser-based sensor should not be affected by changes in the environment and in working conditions.

If the main features of the laser patterns projected on the surface of the products under inspection are known, changes in the environment or in working conditions can be detected, and the system can be automatically set up to avoid their influence on the final measurements.

Defining the features of laser patterns projected onto the surface of rails in harsh industrial environments, like a rolling mill, seems to be an unaffordable task. Steel rail surfaces are composed of a mixture of diffuse and reflective areas. In addition, slag and dust deposited on the surface affect the surface reflectivity. Therefore, the approach proposed in this paper characterizes laser patterns based on thousands of rails inspected previously by a rail PMS while being manufactured in a rolling mill. Raw images acquired by this system are processed to characterize the laser patterns according to the procedures described below.

Experiments show that the uncertainty in measurements based on laser triangulation techniques is mainly from the lens aperture and the triangulation angle [23]. The lens aperture greatly influences the line width imaged by the camera for a given laser emitter. Although a large aperture to image a wide line is desired, this would lead to laser speckle into the image. The speckle noise [24] arises because, at each point of the image, the light wave amplitudes is the result of summation of contributions from all the scattering points of the object inside one resolution cell of the imaging lens. When the object is rough on a scale comparable to the wavelength of the laser generator, as it happens with rail surfaces due to the milling process, the summation involves random vectors. For some portions of the image these vectors cancel each other, leading to dark speckles, while for other parts of the image they tend to reinforce each other, leading to bright speckles [7].

Next, we describe four features to characterize the laser pattern projected by four laser emitters (using the rail PMS described above) on the surface of a rail. These features are the line width, the line intensity, the coverage ratio, and the overlap distance. Sensors will be designed to measure each of these features, and acquired data will be sent to the manager to act in consequence, as shown in Fig. 1.

A. Line width

The width of a light pattern projected onto the surface of the rail is a key feature for height discrimination —which defines the accuracy of 3D measurement— using the laser triangulation technique. In general, the wider the strip, the more accurate the height measurement. However, a wide laser strip may also be a symptom of overexposition, or unfocused or dirty lenses.

Steger's Gaussian line model [22] is used to compute the line width for all points in the extracted line. The line width is determined for all the light patterns imaged by each camera in all the frames acquired while milling a rail. Therefore, the sensor provides four width values for each rail: w_r^1, w_r^2, w_r^3, and w_r^4, where r is the measured rail. Figure 3(a) shows a portion of the laser line projected onto the surface of a rail, and the points (red and blue crosses) where it is considered to end for the purpose of computing its width.

B. Line intensity

The intensity of the light pattern projected onto the surface of the rail under inspection is another key feature for height discrimination in laser triangulation. The laser intensity indicates the average gray value of the points in the laser line. In the rail PMS used in this work, images are 8-bit grayscale; thus, the line intensity is a value between 0 and 255. This feature can be used to detect image overexposition and underexposition.

The sensor designed to measure the intensity of the light pattern computes the average of the intensity of all the pixels crossed by the normals of the extracted laser points that are nearer than half the line width. The line intensity is computed for all the light patterns imaged by each camera in all the frames acquired while milling a rail. Therefore, the sensor provides four width values for each rail: h_r^1, h_r^2, h_r^3, and h_r^4, where r is the measured rail. Figure 3(b) shows a portion of the laser onto the surface of a rail, highlighting the pixels used by the sensor to compute the line intensity.

C. Coverage ratio

In ideal working conditions, the rail PMS expects a continuous light pattern projected onto the surface of the rail, depicting its profile. However, in real measurement scenarios the surface conditions of the rail and the hostile conditions of the rolling mill atmosphere could lead to discontinuities in the

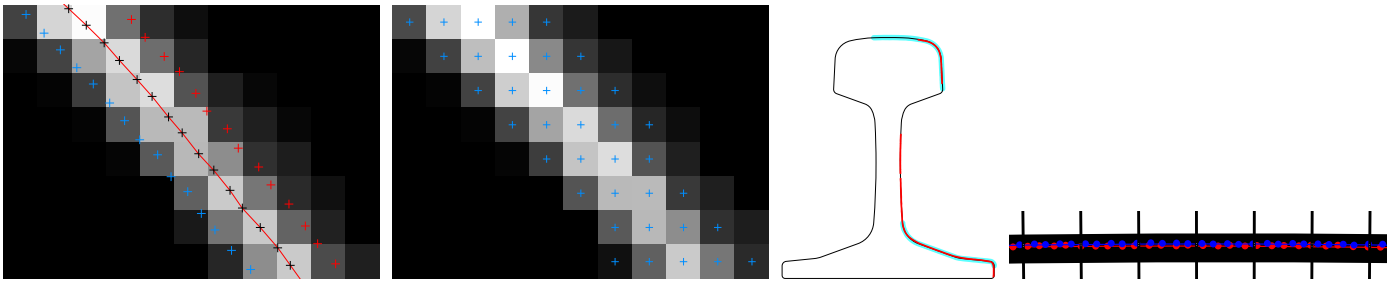

(a) (b) (c) (d)

Fig. 3. Laser characterization: (a) Line width: the laser line (red) and the extracted points are shown (black crosses), superimposed to the raw image, and the points where the line is considered to end ($|x| = w$ in Steger's model) are also depicted (blue and red crosses); (b) line intensity: the pixels that are considered when computing the intensity are marked (blue crosses); (c) coverage ratio: an example of coverage for one of the cameras is shown, where the model primitives that were considered are shown in cyan, while the actual laser line is colored red; (d) overlap distance: part of the head of the rail model (black) is shown, along with the normal vectors (also black, vertical), and both laser lines (red and blue).

light pattern imaged by the system, which will affect further measurement stages.

The sensor designed to measure the coverage ratio of the light pattern at the intersection of the sheet-of-light generated by the laser emitters and the surface of the rail computes the portion of the rail profile that is covered by the laser line. A point cloud that models the rail is built by sampling the primitives (arcs and segments) from certain regions of the rail that are visible to the camera for all rail models. The distance between two consecutive points, measured on the given primitive, is 0.5 mm. Then, a point cloud describing the laser line is built from the extracted line after being undistorted, translated into the world coordinate system, and aligned with the model. A point in the model point cloud, p_m, is considered to be covered if there is a point in the laser line point cloud, p_l, such that $d(p_m, p_l) \leq 1\,mm$, where d is the Euclidean distance between two points. The coverage ratio is computed as the ratio between the number of covered points and the total number of points in the point cloud of the rail model. Figure 3(c) compares the rail model primitives that should be seen by camera C_2 with the laser line as seen by said camera.

D. Overlap distance

The light pattern imaged by the rail PMS should be a continuous line where segments imaged by separated cameras cannot be identified. That is, all the points in the rail point cloud would match the ideal rail profile and, without additional information, points in the areas where laser lines from separated emitters overlap would not be able to be tracked back to their acquisition source.

However, in industrial environments, calibrating the laser triangulation units will incur in certain calibration errors which will affect line overlapping [25]. In addition, although the rail PMS used in this work is installed in a ruggerized housing in the rolling mill —using rubber bushings to isolate vibrations caused by rolling—, the geometry of the system (and hence, line overlapping) could suffer because of the extremely hostile conditions in the mill.

In the rail PMS used in this work, laser lines overlap at four different regions: The lines for cameras C_1 and C_2 overlap at the head arc; the lines for cameras C_1 and C_4 overlap at the rail web; the lines for cameras C_2 and C_3 also overlap at the rail web; and the lines for cameras C_3 and C_4 overlap at the foot. Overlaps at the rail web have been empirically identified as the most unreliable, as laser lines are often weak there, and that region is prone to occlusion. Therefore, only overlaps at the head ('upper overlap distance') and the foot ('lower overlap distance') should be considered for this purpose.

The sensor designed to measure the overlap distance of the segments composing the light pattern fits the laser lines from a pair of cameras to arcs or lines, depending on the region of the rail where they are located. Then, normal vectors of the model at every 1 mm are generated, and the distances between the points where the arcs or lines intersect each of these normal vectors are computed. The computed distances are then averaged. Figure 3(d) shows the appearance of two overlapping laser lines together with the rail model.

IV. Autonomic Computing for Rail Profile Measuring

The expression *autonomic computing* was coined by IBM in 2001 [26]. The term *autonomic* was inspired by the autonomic nervous system, which manages unconscious bodily functions in animals. In an ideal implementation of autonomic principles, an autonomic manager is supposed to implement the so called MAPE-K loop [11]: *Monitor* the managed element, collect and store sensor data; *Analyze* the stored data, identify problems and opportunities for improvement; *Plan* an action or sequence of actions for the managed element to take, using a repository of knowledge which stores models for system behaviour; and *Execute* the plan.

Depending on the degree of application of the principles of autonomic computing, and on the complexity of the system, some policies may be defined [27]: *i*) describe the actions that must be taken when certain conditions are met (rule-based policies); *ii*) describe the values that some properties should have and let the system decide on specific actions (goal-based policies); or *iii*) specify a utility function that must be maximized or minimized (utility function-based policies).

Autonomic computing techniques range from the comparison between the measured values, according to criteria selected by the programmer or user —in which case the manager can be implemented as a rule engine or an expert system [28]—, to the use of machine learning techniques to analyze the measured values during the entire life of the system and apply the results in order to reach high-level goals [27].

Such techniques include neural networks, probabilistic models and combinatorial search [29], depending on the specific self-management feature that is to be implemented.

Apart from classifying autonomic systems according to their architecture and their degree of compliance with IBM's autonomic ideals, a quantitative evaluation of autonomic capabilities may be performed. Self-healing and self-protection capabilities may be measured by fault injection [30], while self-optimization capabilities may be checked by subjecting the system to a quickly varying workload under different conditions.

A. Autonomic machine vision systems

Adding autonomic features to a computer vision system entails analyzing the acquired images in order to determine the state of the imaging devices, the light sources, and the image processing modules. The resulting information may then be used to detect problems, and to optimize the settings of both the computer vision software and the hardware elements, to the extent that they may expose their configuration to the software.

The managed elements of the machine vision system may expose a set of image properties, so that only those properties may be taken into account for self-management purposes, or it may expose the raw images for sensors to extract full potential of raw data. In the latter, the manager would operate as a secondary computer vision system, and consider all the features that may appear in the images.

B. Proposed approach

The approach proposed in this work aims to provide a rail PMS with capabilities to: *i*) automatically detect changes in both the working environment and the operating conditions; and *ii*) warn operators of the rail rolling mill when working conditions indicate that the inspection system is about to provide incorrect measurements. The intervention of operators or technicians is not required for problem diagnosis: it is only needed for specific manual tasks, such as replacing or cleaning the laser emitters, once an alert is notified by the system.

The core of the manager in the proposed approach is an expert system, which is divided into two subsystems: a rule system and a knowledge base. The rule system is based on *if-then* rules, and the knowledge base is built upon the data gathered by the sensors described above to characterize the light pattern used by the PMS.

Generally, expert systems suffer from the knowledge acquisition problem. This problem refers to the difficulties related to obtaining the knowledge that the system must start working with. In this work, we address the knowledge acquisition through a broad experimentation process based on historical data acquired by the rail PMS in several months of operation in a rail rolling mill in many different working conditions.

C. Communication of issues to human operators in the proposed approach

A standardized way to communicate issues to the human operators is required. Such communication should be carried out in three different ways:

1) Events: Alert events may be triggered in order to warn the operator about serious system problems that require immediate action. These include any individual sensor being out of range to such an extent that current measurement results may have no value; or the complete inability to measure rails for any other reason, such as camera trigger failure. The event notifications would state both the cause of the events and the recommended manual action the operators or technicians should perform, such as cleaning the camera lenses or repairing the trigger system.

A set of rules may be used to decide when an alert event should be triggered. Rules can be built by combining two kinds of elements: strategies to compute the range for a given sensor at a given time and strategies to compute the values that will be compared with said range.

The following kinds of range strategies have been considered: *i*) hard limits where values must fall between two predefined numbers; *ii*) percentile limits, where values must fall between two predefined percentiles of the last N sensor values; and *iii*) relative limits, where values must be within a predefined distance of the average of the first N values since the last calibration.

Possible value computation strategies are as follows: *i*) using the last value returned by the sensor; *ii*) using the average of the last N values returned by the sensor, and not returning a value when less than N values are available; and *iii*) fitting a line to the last N sensor values, then using the value at a given point in time, extrapolated from this line.

A tentative set of rules, combining all these strategies, can be seen in Algorithm 1.

2) Reports: System reports may be issued periodically. These reports may include recent sensor values, average and other statistics; overall system health, derived from said values; number of alerts and other events during the period covered by the report; and estimated time until sensor values get out of range. System reports are intended to provide a quick summary in order for operators to check that the system is healthy, and allow them to perform preventive maintenance when needed.

3) Dashboard: A sensor dashboard would be displayed on demand, and show all the information that would appear in a system report; current and historical sensor data; all the recorded alerts and other events, including maintenance events, and all the generated system reports. The sensor dashboard is intended to expose all the available sensor information in order to allow operators to investigate system failures or predict future issues. The dashboard is mostly intended as a fallback, to allow operators to find issues that the manager cannot adequately detect; and also as a way to assess the quality of the feedback returned by the autonomic manager, and fix any issues caused by the manager itself.

V. Experimental results

Sensors were implemented to measure the light pattern features described before. In order to determine their usefulness at detecting issues in the operation of the PMS, the sensors were applied to the raw image database of each of the 52756 rails that were measured by the PMS in the rail rolling mill between January 1, 2017 and December 31, 2017. This database contains more than 79,12 million images.

Algorithm 1 Rule system. *intensity*, *width*, *coverage* and *overlap* lists contain the average values of each sensor for all triangulation units and all measured rails. The function described here should be called every time a new rail is measured.

function CHECKHEALTH(*intensity*, *width*, *coverage*, *overlap*)
  for all $c \in 1..4$ **do**
    if not $(1.75 \leq width_c[\textbf{last}] \leq 3)$ **then** ▷ Rule W.1.
      ALERT($width_c$, "hardLimit")
    end if
    $recent \leftarrow width_c[\textbf{last} - 4999..\textbf{last}]$
    if not $(recent_{10\,\%} \leq \textbf{avg}(width_c[\textbf{last} - 249..\textbf{last}]) \leq recent_{95\,\%})$ **then** ▷ Rule W.2.
      ALERT($width_c$, "movingAverage")
    end if
    $line \leftarrow$ LINEARINTERPOLATION($width_c[\textbf{last} - 249..\textbf{last}]$)
    if not $(1.75 \leq line(\textbf{now} + 7\ \textbf{days}))$ **then** ▷ Rule W.3.
      ALERT($width_c$, "prediction")
    end if
    if not $(50 \leq intensity_c[\textbf{last}] \leq 240)$ **then** ▷ Rule I.1.
      ALERT($intensity_c$, "hardLimit")
    end if
    $recent \leftarrow intensity_c[\textbf{last} - 4999..\textbf{last}]$
    if not $(recent_{10\,\%} \leq \textbf{avg}(intensity_c[\textbf{last} - 249..\textbf{last}]) \leq recent_{90\,\%})$ **then** ▷ Rule I.2.
      ALERT($intensity_c$, "movingAverage")
    end if
    $line \leftarrow$ LINEARINTERPOLATION($intensity_c[\textbf{last} - 249..\textbf{last}]$)
    if not $(50 \leq line(\textbf{now} + 7\ \textbf{days}))$ **then** ▷ Rule I.3.
      ALERT($intensity_c$, "prediction")
    end if
    if not $(0.9 \leq \textbf{avg}(coverage_c[\textbf{last} - 249..\textbf{last}]))$ **then** ▷ Rule C.1.
      ALERT($coverage_c$, "movingAverage")
    end if
  end for
  for all $d \in 1..2$ **do**
    if not $(\textbf{avg}(overlap_d[\textbf{last} - 249..\textbf{last}]) \leq 0.25)$ **then** ▷ Rule O.1.
      ALERT($overlap_d$, "movingAverage")
    end if
    $lastCalib \leftarrow$ LASTCALIBRATION($overlap_d$)
    $avgLastCalib \leftarrow \textbf{avg}(overlap_d[lastCalib..lastCalib + 249])$
    $avgValue \leftarrow \textbf{avg}(overlap_d[\textbf{last} - 249..\textbf{last}])$
    $len \leftarrow \textbf{count}(overlap_d)$
    if $lastCalib + 249 \leq len$ **and not** $(avgValue \leq avgLastCalib + 0.05)$ **then** ▷ Rule O.2.
      ALERT($overlap_d$, "movingAverageDeviation")
    end if
  end for
end function

A. Line width

Figure 4(a) shows the average line width for every camera for the rails that were considered (although only one data point is shown out of every 100, to avoid cluttering). Results for cameras C_1 and C_2 (the upper cameras) appear to be largely stable. However, line widths seem to degrade in a monotonic manner for camera C_3, and reset to their original values from time to time (mostly when the camera is cleaned). Camera C_4 appears to have thicker lines than all the other cameras, and exhibits a deviation that falls between the deviations of cameras C_1 and C_2 and that of Camera C_3.

Table I confirms that most alert events would be triggered for cameras C_3 and C_4. Rule W.3 (prediction) events are more common for camera C_3, correctly detecting the degradation of its line width.

B. Line intensity

Figure 4(b) shows the average line intensity for every camera, for the rails that were considered. Again, laser intensity can be seen not to degrade at all for the upper cameras, C_1 and C_2. However, for the lower cameras, especially camera C_4, the intensity degrades continuously, and it only improves when the lenses are cleaned, the laser emitters are replaced or the exposure time is increased. As such, the observed degradation may be attributed to the accumulation of oil and steel particles, which would mainly affect the lower cameras and laser emitters.

Again, Table I confirms that most alert events would be triggered for the lower cameras, C_3 and C_4.

Figure 5 depicts the behavior of the laser line intensity for one of the cameras (camera C_4) during a single month (May

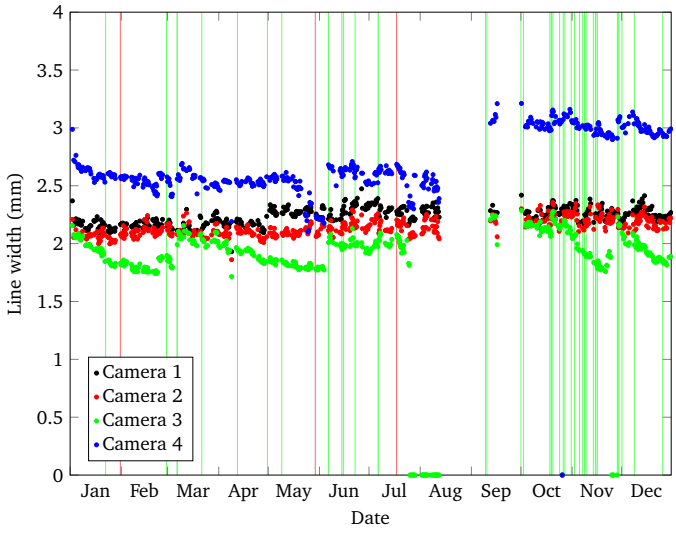

(a)

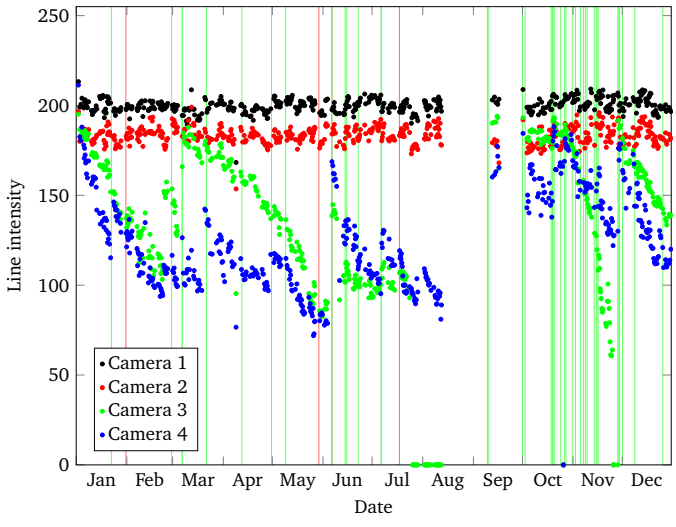

(b)

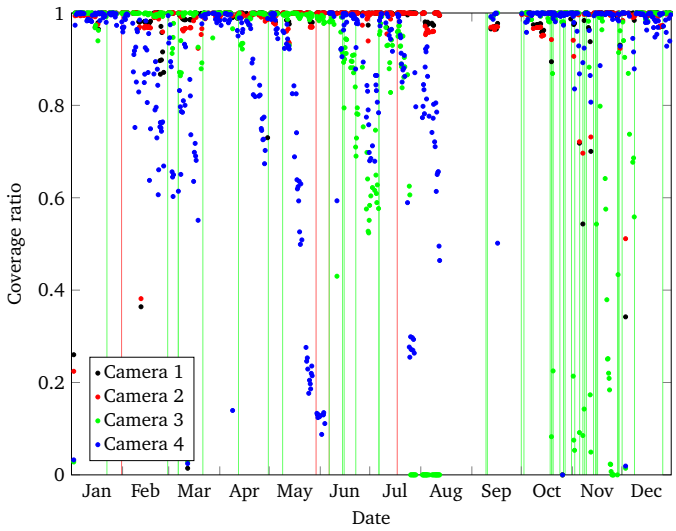

(c)

Fig. 4. Results of some of the sensors for the first rail that was measured by the production system every day from January 1, 2017 to December 31, 2017: (a) Line width; (b) line intensity; (c) coverage ratio. A green line denotes a calibration event. A red line signals that production stopped for 48 hours or longer. Only one out of every 100 data points is shown.

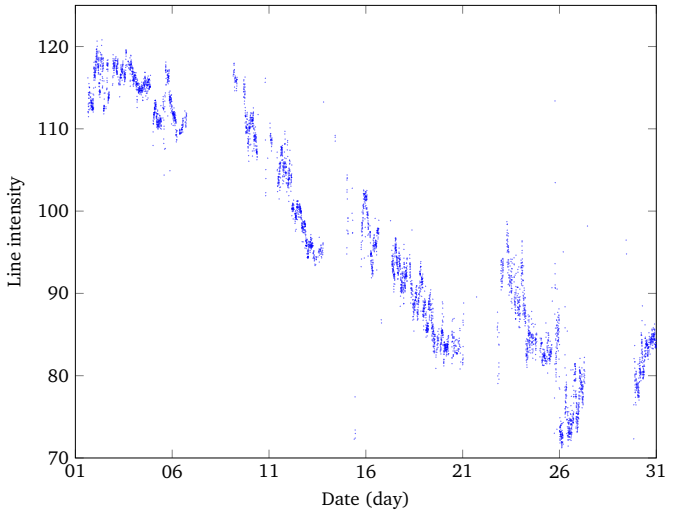

Fig. 5. Average laser line intensity for camera C_4, for each of the 5233 rails that were measured during May 2017.

2017). The plot is jagged, with sudden, very steep variations of up to about 10 intensity units, which contrast with a slower downward trend.

Although they are not pictured here, plots for the other cameras (especially camera C_3) are similarly jagged. These upward slopes came as a surprise: intensity was expected to degrade almost monotonically, and seldom increase except for maintenance events.

One possible conjecture is that the laser intensity follows a daily cycle, even though lighting conditions are controlled inside the facility where the PMS is located, and there is no access to natural light. For all the rails that were measured during May 2017, Figure 6 depicts the difference between their average laser line intensity and the daily average. No patterns are apparent. Additionally, the median difference (as described before) for each 15 minute interval was computed for the rails measured during May 2017 and for all the rails measured during the year. No correlation was found. Therefore, laser line intensity does not appear to follow a daily cycle, and the reasons for its behavior are still unknown.

C. Coverage ratio

Figure 4(c) shows the average coverage ratio for every camera, for the rails that were considered. Cameras C_1 and C_2 can be seen to have a stable coverage ratio, with only a small number of outliers. However, cameras C_3 and C_4, and especially the latter, can be seen to degrade very quickly. The results of this sensor are very similar, at least in tendency, to those of the previous ones.

Consistently with results from the other sensors, Table I shows that alert events related to the coverage ratio are more common for the lower cameras.

D. Overlap distance

Figure 7 shows the average value of both upper and lower overlap distance for the rails that were measured during 2017.

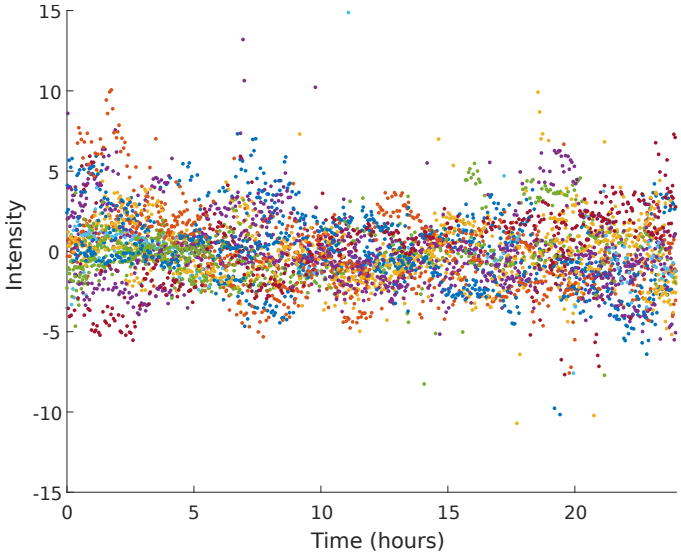

Fig. 6. Evolution of the line intensity for camera C_4 during the day. For each of the 5233 rails that were measured during May 2017, the difference between its average intensity and the daily average is shown. Rails that were measured during the same day are depicted in the same color.

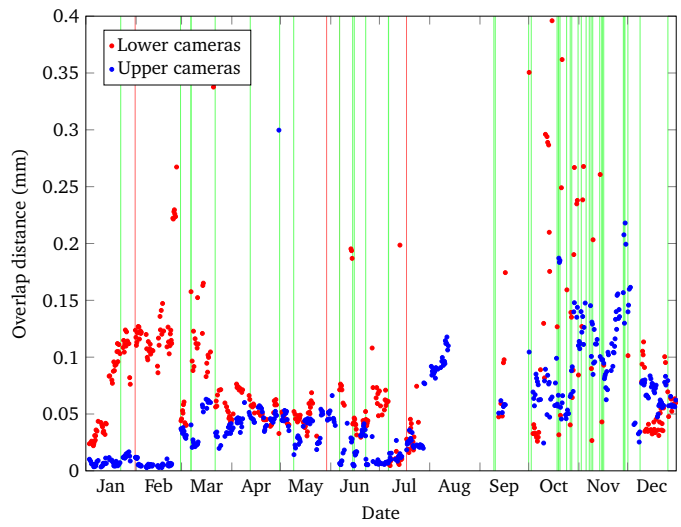

Fig. 7. Lower (red) and upper (blue) overlap distances. A green line denotes a calibration event. A red line signals that production stopped for 48 hours or longer. Only one out of every 100 data points is shown.

The lower cameras consistently have larger values, as well as a higher deviation.

Line distances were expected to slowly increase after every calibration. However, they seem to be mostly stable, excluding the outliers; they even show a slight tendency to decrease at some points.

Alert events are more common for the lower cameras here, as with the other sensors, even though the kinds of issues this sensor is intended to detect (need for recalibration) are different from those detected by the other ones (mostly degraded laser emitters and dirty camera lenses).

TABLE I. PERCENTAGE OF RAILS THAT TRIGGERED ALERT EVENTS.

Rules	C_1	C_2	C_3	C_4	Overall
W.1	0.53	0.52	8.26	18.03	6.83
W.2	9.67	7.93	23.62	14.63	13.96
W.3	5.53	10.86	32.00	2.16	12.64
Any width rule	13.83	17.24	45.46	31.41	26.99
I.1	0.53	0.50	7.31	0.46	2.20
I.2	12.50	9.03	37.04	23.61	20.55
I.3	0.80	0.74	12.74	7.19	5.37
Any intensity rule	12.56	9.10	44.94	28.79	23.85
Coverage rule	3.91	2.72	27.23	35.65	17.38
O.1		1.68		16.96	9.32
O.2		7.80		31.38	19.59
Any overlap rule		8.31		33.34	20.83

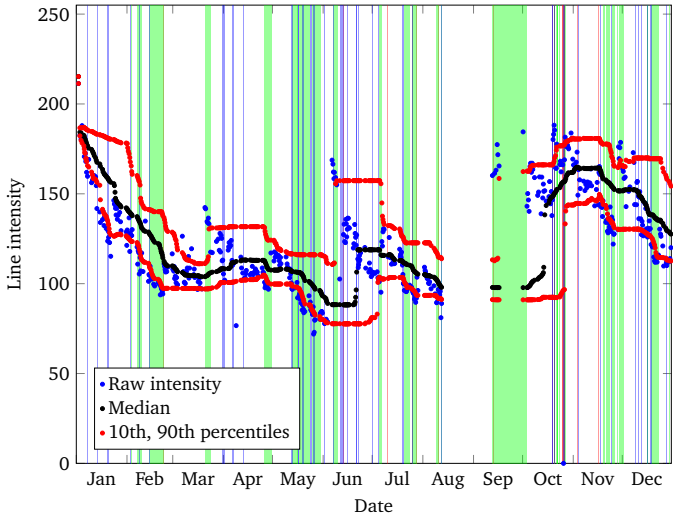

Fig. 8. Line intensity for camera C_4. The median and the 10th and 90th percentiles are also shown. Vertical bars designate the regions where one or more contiguous rails triggered one of the alert rules: red bars for rule I.1 (hard limits), green bars for rule I.2 (percentile limits), and blue bars for rule I.3 (relative limits). Only one out of every 100 data points is shown.

E. Alert events

Based on the outputs provided by these sensors, the autonomic manager of the PMS is set up. When the PMS is in operation, this manager will provide reports for the human operators of the rail rolling mill as described in Sect. IV. Future versions of the system may use this output to configure itself until it is properly maintained by human operators, if required.

Using the tentative rules described in Algorithm 1, the percentage of rails that triggered an alert event for each sensor and individual rule was computed, and is shown in Table I.

Figure 8 depicts the laser intensity for all the rails that were measured during 2017, as seen by one of the cameras (camera C_4), along with the alert events that were triggered. As shown in Table I, percentile-based triggers (rule I.2, green) are the most common, followed by relative triggers (rule I.3, blue). The line intensity seldom reaches the hard limits (rule I.1, red). Additionally, Rule I.2 events often occur in longer bursts.

VI. DISCUSSION

The expert system described above has shown its potential to detect issues in the triangulation units (and, to a limited extent, to predict them): not just by determining whether the

results are inside a predefined range but also in a number of additional ways that take into account the variability of sensor data, and the tendency it shows. For instance, the approach proposed in this paper has warned technicians of the rail rolling mill that working conditions of triangulation units of cameras C_3 and C_4 change frequently, making them operate in worse conditions than triangulation units of cameras C_1 and C_2 (see Table I and Figure 4).

The rules shown here are just tentative, and refinement is needed. Strict rules were used in the previous experiments in order to communicate any potential issue in the rail profile measurement system, but rules for the production environment should be more permissive, so that each alert event corresponds to an actual need for maintenance.

In order to design self-healing features, a better understanding of the influence of different parameters on the results would be required. This could be achieved by performing a parameter-space search on the parameters related to laser line extraction, camera calibration, profile alignment and dimension measurement. Some of them may be set independently for each of the cameras, as the laser emitters employ different wavelengths, and may be exposed to different levels of degradation, as suggested by Figure 4. Additionally, synthetic or modified images may be needed in order to model the influence of the parameters on system behavior in extreme situations (e.g. by darkening or lightening them, or removing parts of the laser lines). This should be greatly parallelizable, so a High Performance Computing cluster would help in performing the search and testing different strategies.

VII. Conclusions

Rail profile measurement systems in rolling mills are crucial inspection equipment to guarantee compliance with rail standards prior rail track construction. Systems based on laser triangulation may suffer from degradation of hardware components of the image acquisition subsystem and from environmental conditions inherent to hostile environments.

In this work, we added autonomic computing capabilities to create a self-aware rail profile measurement system in a rail rolling mill, based on characterizing the laser patterns projected onto the surface of the rails by means of a set of proposed sensors. The output provided by these sensors is used to set up an expert system that is able to warn process computers and operators of the rail rolling mill.

Future work will involve changing the behavior of the profile measurement system using the output provided by the expert system, to guarantee proper operation or schedule corrective actions for preventive maintenance.

Acknowledgment

This work was partially funded by project TIN2014-56047-P of the Spanish National Plan for Research, Development and Innovation, by project FUO-EM-372-14 and by the "Severo Ochoa" program of the Asturian Regional Government under grant PA-17-PF-BP16009.

Parts of this work were performed (application HPC17UE41N) under the Project HPC-EUROPA3 (INFRAIA-2016-1-730897), with the support of the EC Research Innovation Action under the H2020 Programme. Author Álvaro F. Millara gratefully acknowledges the support of Prof. Robert Fisher and the computer resources and technical support provided by the Edinburgh Parallel Computing Centre at the University of Edinburgh.

References

[1] B. Deo and R. Boom, *Fundamentals of Steelmaking Metallurgy*. Prentice Hall, 1993.

[2] M. Papaelias, C. Roberts, and C. Davis, "A review on non-destructive evaluation of rails: State-of-the-art and future development," in *Proceedings of the Institution of Mechanical Engineers Part F Journal of Rail and Rapid Transit*, vol. 222, no. 4, 2008, pp. 367–384.

[3] P. Bernal, D. Garcia, and R. Usamentiaga, "Rail flatness measurement method based on virtual rules," *IEEE Transactions on Industry Applications*, vol. 53, no. 4, pp. 4116–4124, 2017.

[4] F. J. delaCalle, D. F. Garcia, and R. Usamentiaga, "Inspection system for rail surfaces using differential images," *IEEE Transactions on Industry Applications*, 2018.

[5] J. Molleda, R. Usamentiaga, A. F. Millara, D. F. Garcia, P. Manso, C. M. Suarez, and I. Garcia, "A profile measurement system for rail quality assessment during manufacturing," *IEEE Transactions on Industry Applications*, vol. 52, no. 3, 2016.

[6] W. Lohry, V. Chen, and S. Zhang, "Absolute three-dimensional shape measurement using coded fringe patterns without phase unwrapping or projector calibration," *Optics Express*, vol. 22, no. 2, pp. 1287–1301, 2014.

[7] H. Baribeau and M. Rioux, "Influence of speckle on laser range finders," *Applied Optics*, vol. 30, no. 20, pp. 2873–2878, 1991.

[8] N. VanGestel, S. Cuypers, P. Bleys, and J. P. Kruth, "A performance evaluation test for laser line scanners on CMMs," *Optics and Lasers in Engineering*, vol. 47, no. 3-4, pp. 336–342, 2009.

[9] F. Xi, Y. Liu, and H.-Y. Feng, "Error compensation for three-dimensional line laser scanning data," *The International Journal of Advanced Manufacturing Technology*, vol. 18, no. 3, pp. 211–216, 2001.

[10] J. Kephart and D. Chess, "The vision of autonomic computing," *Computer*, vol. 36, no. 1, pp. 41–50+4, 2003.

[11] M. C. Huebscher and J. A. McCann, "A survey of autonomic computing - degrees, models, and applications," *ACM Computing Surveys*, vol. 40, no. 3, 2008.

[12] M. R. Nami and K. Bertels, "A survey of autonomic computing systems," in *3rd International Conference on Autonomic and Autonomous Systems, ICAS'07*, 2007, pp. 26–30.

[13] A. F. Millara, J. Molleda, R. Usamentiaga, and D. F. Garcia, "Profile measurement of rails in rolling mills: integrating autonomic computing capabilities," in *Proc. of 2018 IEEE Industry Applications Society Annual Meeting, IAS 2018*. IEEE, 2018, pp. 1–8.

[14] F. Chen, G. Brown, and M. Song, "Overview of three-dimensional shape measurement using optical methods," *Optical Engineering*, vol. 39, no. 1, pp. 10–22, 2000.

[15] Y. Frauel, E. Tajahuerce, O. Matoba, A. Castro, and B. Javidi, "Comparison of passive ranging integral imaging and active imaging digital holography for three-dimensional object recognition," *Applied Optics*, vol. 43, no. 2, pp. 452–462, 2004.

[16] Q. Tang, "Railway track geometry realtime inspection system," in *Proceedings of the IEEE Instrumentation and Measurement Technology Conference*, 1992, pp. 656–660.

[17] C. Alippi, E. Casagrande, F. Scotti, and V. Piuri, "Composite real-time image processing for railways track profile measurement," *IEEE Transactions on Instrumentation and Measurement*, vol. 49, no. 3, pp. 559–564, 2000.

[18] Z. Liu, J. Sun, H. Wang, and G. Zhang, "Simple and fast rail wear measurement method based on structured light," *Optics and Lasers in Engineering*, vol. 49, no. 11, pp. 1343 – 1351, 2011.

[19] J. Molleda, R. Usamentiaga, and D. Garcia, "On-line flatness measurement in the steelmaking industry," *Sensors*, vol. 13, no. 8, pp. 10 245–10 272, 2013.

[20] M. Levoy, S. Rusinkiewicz, M. Ginzton, J. Ginsberg, K. Pulli, D. Koller, S. Anderson, J. Shade, B. Curless, L. Pereira, J. Davis, and D. Fulk, "The digital michelangelo project: 3d scanning of large statues," in *Proceedings of the ACM SIGGRAPH Conference on Computer Graphics*. ACM Press/Addison-Wesley Publishing Co. New York, NY, USA, 2000, pp. 131–144.

[21] R. Usamentiaga, J. Molleda, and D. Garcia, "Fast and robust laser stripe extraction for 3d reconstruction in industrial environments," *Machine Vision and Applications*, vol. 23, pp. 179–196, 2012.

[22] C. Steger, "Unbiased extraction of lines with parabolic and gaussian profiles," *Computer Vision and Image Understanding*, vol. 117, p. 97âĂŞ112, 02 2013.

[23] R. G. Dorsch, G. Hausler, and J. M. Herrmann, "Laser triangulation: Fundamental uncertainty in distance measurement," *Applied Optics*, vol. 33, no. 7, pp. 1306–1314, 1994.

[24] W. Dremel, G. Hausler, and M. Maul, "Triangulation with large dynamical range," in *Proc. SPIE*, vol. 0665, 1986, pp. 182–187.

[25] R. Usamentiaga, D. Garcia, and F. delaCalle, "Real-time inspection of long steel products using 3-d sensors: Calibration and registration," *IEEE Transactions on Industry Applications*, vol. 54, no. 3, pp. 2955–2963, 2018.

[26] A. G. Ganek and T. A. Corbi, "The dawning of the autonomic computing era," *IBM Systems Journal*, vol. 42, no. 1, pp. 5–18, 2003.

[27] J. O. Kephart, "Research challenges of autonomic computing," in *27th International Conference on Software Engineering, ICSE05*, 2005, pp. 15–22.

[28] D. Agrawal, S. Calo, J. Giles, K.-W. Lee, and D. Verma, "Policy management for networked systems and applications," in *2005 9th IFIP/IEEE International Symposium on Integrated Network Management, IM 2005*, vol. 2005, 2005, pp. 455–468.

[29] D. A. Menasce and M. N. Bennani, "On the use of performance models to design self-managing computer systems," in *Proc. 2003 Computer Measurement Group Conf*, 2003, pp. 7–12.

[30] T. K. Lau and P. K. L. Shum, "Quantitative measurement of the autonomic capabilities of computing systems," U.S. Patent 7.539.904-B2, 2005.